A new integration method of Hamiltonian systems by symplectic maps

1999 J. Phys. A: Math. Gen. 32 2745

(http://iopscience.iop.org/0305-4470/32/15/004)

J. Phys. A: Math. Gen. **32** (1999) 2745–2766. Printed in the UK PII: S0305-4470(99)98794-2

A new integration method of Hamiltonian systems by symplectic maps

S S Abdullaev

Institut für Plasmaphysik, Forschungszentrum Jülich GmbH, EURATOM Association, Trilateral Euregio Cluster, D-52425 Jülich, Germany

Received 29 October 1998, in final form 20 January 1999

Abstract. A perturbation theory is developed for constructing stroboscopic and Poincaré maps for Hamiltonian systems with a small perturbation. It is based on a canonical transformation by which the evolution becomes unperturbed during the entire period while all perturbations are acting instantaneously during one kick per period. Matching of solutions before and after the kicks establishes a symplectic map which exactly describes the evolution. The generating function associated with this map satisfies the Hamilton–Jacobi equations. The solution of this equation is found in first order of perturbation theory. It is shown that the map reproduces correctly Poincaré sections and statistical properties of typical orbits. It is shown that the well known perturbed twist mapping and, in particular, the standard map may be obtained from the symmetric map as an approximation. The method is also applied to construct Poincaré maps at arbitrary sections of the phase space. In particularly, the maps describing a motion near the separatrix are derived.

1. Introduction

A Poincaré return map is a powerful method to analyse multidimensional dynamic systems, especially to study dynamic chaotic systems [1–4]. It replaces the dynamics of a continuous time system by a discrete one (a map). The map has several important advantages for the study of dynamical systems. First of all it reduces dimensions of the system at least by one. It allows one to visualise a dynamical system at certain sections (Poincaré sections) of the phase space, displaying the global dynamics of it. The Poincaré map clarifies the formulation of many concepts of continuous systems. For example, the determination of orbit stability is simply reduced to a study of the stability of a fixed point.

Many fundamental models of physics and mechanics are Hamiltonian systems. For Hamiltonian systems Poincaré maps should be presented as symplectic mappings [3, 5, 6]. Symplectic mappings have been extensively used in a variety of problems of physics and mechanics, like wave–particle interactions [7, 8], magnetic field structure in magnetic confinement devices [9–15], transport and mixing in fluids [16–20], particle motion in accelerators [21], and in long-time evolution of the solar system [22–26]. From the computational point of view they run much faster than finite element based solutions of differential equations.

In order to construct Poincaré maps general orbits of the system are necessary. They may be directly obtained by numerical integration of the equations of motion, which usually requires long computer times. Approximate maps may be also established using perturbation and averaging methods [2, 4]. For example, in [3] a Poincaré map is constructed for a two-degree-of-freedom Hamiltonian system by means of two-dimensional symplectic maps, named

0305-4470/99/152745+22$19.50

perturbed twist maps. However, one should note that except for some specific cases, there are no rigorous derivations of symplectic maps from the equations of motion, and that the existing methods of their derivation are not quite satisfactory. They are mainly based on replacing a perturbation by a series of delta functions, and subsequently integrating the equations along them [7, 14, 22]. Because the integration procedure of a delta function is not well defined, one can obtain different forms of maps depending on the asymptotic representation of the delta function. In particular, as was recently shown in [27], its symmetric representation gives rise to a symmetric form of the map which describes a Hamiltonian system more closely than the perturbed twist map. The latter does not conserve the symmetry of Hamiltonian systems with respect to the simultaneous change of the signs of time and Hamiltonian, i.e. $t \to -t$, $H \to -H$.

From the derivation it is also not clear how the map variables are related to those of the continuous system. Usually these variables are simply identified. Any difference between them is important because, as was asserted in [26], it is responsible for 'spurious oscillations in energy and state variables'.

In this paper we develop a new rigorous method for constructing Poincaré maps for Hamiltonian systems. It is a new version of the Poincaré–von-Zeipel perturbation theory, and consists of a regular procedure which reduces the evolution of continuous systems to symplectic mappings.

The perturbation methods of the classical and celestial mechanics are mainly based on the averaging principle (see, e.g., [2,3,5,28,29]). The averaging procedure is usually implemented by a change of variables in the perturbed equations of motion that eliminates fast phases in the equations. In Hamiltonian systems such a change of variables ought to be canonical. The averaged equations are usually easier to study than the original ones.

The idea behind the method described here is somewhat similar, and it intends to find a change of variables in the perturbed equations of motion such that they are easier to integrate. One way to accomplish this is to eliminate the perturbation, which is the main obstacle for the integrability. Generally such a change of variables does not exist globally. Nevertheless one can find a transformation of variables which eliminates the perturbation in certain time intervals. This may be implemented by a transformation of variables which adds an infinite number of fast phases to the perturbed part of the equations, in contrast to the averaging procedure which eliminates fast phases. With this procedure the evolution becomes unperturbed during the entire period, and all perturbations act instantaneously as kicks at the time instants where phases are multiple to 2π. The relation between solutions before and after kicks may be found by the inverse transformation to the old variables using the continuity of the system. This relation allows us to establish a symplectic mapping describing the evolution in one period of perturbation.

The idea of adding fast phases in Hamiltonian equations in order to reduce a continuous system to a symplectic mapping has first been used by J Wisdom in [22] for studying the long-term evolution of the solar system. This mapping method was later generalized in [23–25]. The method is based on adding high-frequency terms in equations of motion which are chosen such that the perturbed Hamiltonian becomes a series of time-periodic delta functions. The behaviour of the system between delta functions is determined by the unperturbed Hamiltonian, and the effects of delta kicks are found by integrating the system across the delta functions. The justification of the method is based on the averaging principle, i.e., on the fact that if high-frequency terms do not contribute significantly to the evolution, adding these terms also does not affect the system significantly. The fact that the variables in the equations and the ones in the mappings are not identical was noticed in [26]. In order to relate these variables, so-called symplectic correctors were introduced by a Lie formalism. This mapping approach has been

successful in the study of the dynamics of the solar system for very long timescales. Although this symplectic mapping method is much faster than conventional symplectic integrators, there are several serious shortcomings of the method.

First of all, the introduction of time-periodic delta functions for the autonomous (explicitly time-independent) system leads to fluctuations in the total energy of the system, which ought to be an invariant. Correctors, introduced in [26] in order to take the difference between mapping variables and the ones of the original system into account, decrease fluctuations of energy but create a secular drift of the energy. Secondly, the transformation from the variables of the system to the mapping variables, given by the Lie generating function at the first order of the perturbation parameter, is not symplectic. On long timescales this may lead to deviations of the system from true trajectories.

The mapping in this paper appears as a result of the regular procedure of the symplectic transformation of variables in Hamiltonian equations. This procedure exactly replaces the dynamics of Hamiltonian systems by the symplectic mapping of a certain form. Generating functions associated with the map satisfy the Hamilton–Jacobi equations, solutions of which may be found using perturbation theory.

The content of this paper is the following. In section 2 we introduce a canonical coordinate transformation in the perturbed Hamiltonian system which eliminates the perturbation during the entire period, and construct a symmetric symplectic map describing the evolution of the system during one period of the perturbation. The relation between the symmetric symplectic map and the perturbed twist mapping is discussed in section 3. The perturbation theory to analyse the Hamilton–Jacobi equation for a generating function is presented in section 4, and its solution is found in the first order of perturbation theory. Comparison of the symmetric mapping with numerical computations is presented in section 5 for the simplified model of perturbed magnetic field lines in tokamaks. The standard Hamiltonian and the associated standard map are studied in section 6. A construction of the Poincaré map at the arbitrary cross-section of the phase space is presented in section 7. In section 8 we derive the map describing of the motion near the separatrix. In particular, derivations of the separatrix map and the shifted separatrix map are given. The new mapping method to study Hamiltonian systems is discussed in the concluding section 9.

2. Canonical transformation and a symmetric symplectic mapping

Consider a Hamiltonian system of N degrees of freedom in a finite domain of the phase space ($q = (q_1, \ldots, q_N)$, $p = (p_1, \ldots, p_N)$). Suppose that in the absence of perturbation the system is completely integrable, and its trajectories lie on n-dimensional tori. Then one can introduce action-angle variables (I, ϑ): $I = (I_1, \ldots, I_N)$, $\vartheta = (\vartheta_1, \ldots, \vartheta_N)$, (mod 2π). The dynamics of the system is determined by the unperturbed Hamiltonian $H_0(I)$:

$$I = \text{const} \qquad \vartheta = \vartheta^{(0)} + \omega(I)t \tag{1}$$

where $\omega(I) = \partial H_0/\partial I$ are frequencies.

Suppose that a small time-periodic perturbation affects the system. The perturbed system is described by the Hamiltonian $H = H_0(I) + \epsilon H_1(I, \vartheta, t)$, which is 2π-periodic in ϑ and t:

$$\frac{\mathrm{d}I}{\mathrm{d}t} = -\epsilon\frac{\partial H_1}{\partial \vartheta} \qquad \frac{\mathrm{d}\vartheta}{\mathrm{d}t} = \omega(I) + \epsilon\frac{\partial H_1}{\partial I} \tag{2}$$

where ϵ is a small dimensionless perturbation parameter ($\epsilon \ll 1$). Furthermore, we suppose that $H_0(I)$ and $H_1(I, \vartheta, t)$ are sufficiently smooth functions, and the trajectories $(I(t), \vartheta(t)$ are continuous at any time.

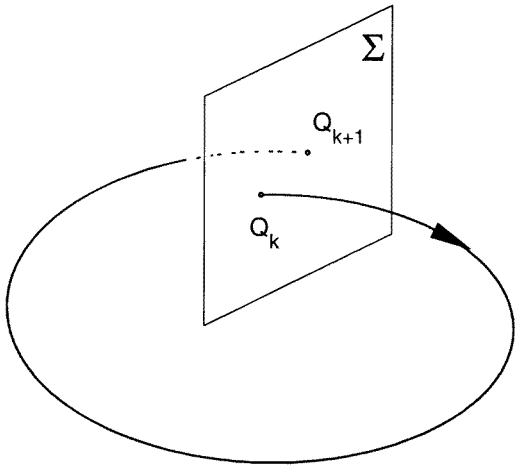

Figure 1. Sketch of Poincaré section and Poincaré map.

Let us first recall a definition of a Poincaré map. In general, trajectories lie in a $(2N+1)$ dimensional subspace of the extended $(2N+2)$ dimensional phase space (ϑ, t, I, H). Consider a $(2N+1)$ dimensional cross-section Σ which is transversally crossed by trajectories as shown in figure 1. Let Q_k be an intersection point of the section by a trajectory. Then the map that associates the point Q_k with the next crossing point Q_{k+1} is a Poincaré map. It is a $2N$-dimensional map.

In order to construct a Poincaré map an appropriate cross-section should be chosen. The choice of the cross-section depends on the specific features of the problem. It is convenient to take a section $\vartheta_i = \text{const}$ where the given angle variable ϑ_i is a constant for each Poincaré section. In particular, the cross-section may be located at periodic time instants $t_k = 2\pi k$ $(k = 0, \pm 1, \pm 2)$. In the latter case we have a stroboscopic map. In this section we construct a stroboscopic map, i.e. $(\vartheta_k, I_k) \to (\vartheta_{k+1}, I_{k+1})$, where $\vartheta_k = \vartheta(t_k)$, $I_k = I(t_k)$. A construction of a Poincaré map at the cross-sections $\vartheta_i = \text{const}$ will be considered in section 7.

Suppose that there exists a canonical transformation of variables $(I, \vartheta) \to (J, \Theta)$:

$$\begin{aligned} I &= J + \epsilon \frac{\partial S(J, \vartheta, t)}{\partial \vartheta} \\ \Theta &= \vartheta + \epsilon \frac{\partial S(J, \vartheta, t)}{\partial J} \end{aligned} \tag{3}$$

given by the generating function $F = J\theta + \epsilon S(J, \theta, t)$ of the mixed old and new variables transforming the Hamiltonian H to the new Hamiltonian $\mathcal{H}$ of the form

$$\begin{aligned} &\mathcal{H} = \mathcal{H}_0(J, \epsilon) + \epsilon \mathcal{H}_1(J, \Theta, t, \epsilon) \\ &\mathcal{H}_1(J, \Theta, t, \epsilon) = \mathcal{H}_1(J, \Theta, \epsilon) \sum_{n=-\infty}^{\infty} \cos nt = 2\pi \mathcal{H}_1(J, \Theta, \epsilon) \sum_{k=-\infty}^{\infty} \delta(t - t_k) \end{aligned} \tag{4}$$

where $J = (J_1, \ldots, J_N)$ and $\Theta = (\Theta_1, \ldots, \Theta_N)$. The transformation (3) eliminates the perturbation in the time intervals $t_k < t < t_{k+1}$. The evolution of the new variables (J, Θ) in these time intervals is then determined by the unperturbed Hamiltonian $\mathcal{H}_0(J, \epsilon)$:

$$\begin{aligned} J(t) &= J_{k+0} \\ \Theta(t) &= \Theta_{k+0} + (t - t_k)\Omega(J_{k+1-0}, \epsilon) \end{aligned} \tag{5}$$

where $\Omega(J,\epsilon) = \partial\mathcal{H}_0(J,\epsilon)/\partial J$ is a motion frequency in the new variables. In particular, we have

$$\begin{aligned} J_{k+1-0} &= J_{k+0} \\ \Theta_{k+1-0} &= \Theta_{k+0} + 2\pi\,\Omega(J_{k+1-0},\epsilon). \end{aligned} \tag{6}$$

In (5) and (6) the following notations are used: $J_{k\pm0} = J(t_k \pm 0)$, $\Theta_{k\pm0} = \Theta(t_k \pm 0)$.

However, the new variables (J,Θ) are not defined at the time instants t_k. After passing the time $t = t_k$, the trajectory $(J(t),\Theta(t))$ discontinuously jumps to the new orbit. However, due to smoothness of the old Hamiltonian function, the trajectory of the system in the old variables (I,ϑ) are continuous at any time. This fact may be used to find jumps of the new variables $(J(t),\Theta(t))$ after the trajectory passes t_k. Indeed, one can apply the canonical transformation (3) connecting the old (I,θ) and new (J,Θ) variables while the trajectory approaches t_k from the both directions, i.e. $t \to t_k \pm 0$. One should note that the generating function $S(J,\vartheta)$ is a discontinuous function of t at $t = t_k$. At the limits $t \to t_k \pm 0$, from (3) we have

$$\begin{aligned} I_k &= J_{k\pm0} + \epsilon\frac{\partial S_\pm(J_{k\pm0},\vartheta_k)}{\partial\vartheta_k} \\ \vartheta_k &= \Theta_{k\pm0} - \epsilon\frac{\partial S_\pm(J_{k\pm0},\vartheta_k)}{\partial J_{k\pm0}} \end{aligned} \tag{7}$$

where $S_\pm(J_{k\pm0},\theta_k) = \lim_{t\to t_k\pm0} S(J,\theta,t)$. Equation (7) determine the relation between the solutions of the new Hamiltonian while the trajectory passes $t = t_k$.

The relationships (7) and the solution (6) allow us to establish a map

$$(I_{k+1},\vartheta_{k+1}) = \hat{T}_s(I_k,\vartheta_k). \tag{8}$$

The mapping may be written as three consecutive symplectic maps $\hat{T}_s = \hat{T}_-\hat{T}_\Omega\hat{T}_+$. The first map $(J_{k+0},\Theta_{k+0}) = \hat{T}_+(I_k,\vartheta_k)$ may be written as

$$\begin{aligned} J_{k+0} &= I_k - \epsilon\frac{\partial S_+(J_{k+0},\vartheta_k)}{\partial\vartheta_k} \\ \Theta_{k+0} &= \vartheta_k + \epsilon\frac{\partial S_+(J_{k+0},\vartheta_k)}{\partial J_{k+0}}. \end{aligned} \tag{9}$$

The second map $(J_{k+1-0},\Theta_{k+1-0}) = \hat{T}_\Omega(J_{k+0},\Theta_{k+0})$ describes the motion of the system between two consecutive sections $t = t_k$ and $t = t_{k+1}$, and according to (6) it may be written as

$$\begin{aligned} J_{k+1-0} &= J_{k+0} \\ \Theta_{k+1-0} &= \Theta_{k+0} + 2\pi\,\Omega(J_{k+1-0},\epsilon). \end{aligned} \tag{10}$$

The last map $(I_{k+1},\vartheta_{k+1}) = \hat{T}_-(J_{k+1-0},\Theta_{k+1-0})$ is

$$\begin{aligned} I_{k+1} &= J_{k+1-0} + \epsilon\frac{\partial S_-(J_{k+1-0},\vartheta_{k+1})}{\partial\vartheta_{k+1}} \\ \vartheta_{k+1} &= \Theta_{k+1-0} - \epsilon\frac{\partial S_-(J_{k+1-0},\vartheta_{k+1})}{\partial J_{k+1-0}}. \end{aligned} \tag{11}$$

Therefore, the described procedure of symplectic transformations reduces the integration of the Hamiltonian system (2) to a mapping, i.e. to algebraic equations. It describes the evolution of $2N$ variables $I = (I_1,\ldots,I_N)$, $\vartheta = (\vartheta_1,\ldots,\vartheta_N)$ over one period of perturbation. The trajectories $(I(t),\vartheta(t))$ at an arbitrary time t between two consecutive time instants t_k and t_{k+1} may be found by using the transformations (3) and equation (5).

The mapping (8) defined by equations (9)–(11) is invariant with respect to the transformation $k \leftrightarrow k+1$, $H \to -H$, the generating functions $S_\pm(J,\vartheta)$ satisfy the condition

$$S_-(J,\vartheta) \to -S_+(J,\vartheta) \qquad \text{for} \quad H \to -H. \tag{12}$$

Further we will call the map (8)–(11) *a symmetric symplectic map* (or simply a symmetric map).

3. The perturbed twist mapping

There is a large class of area-preserving maps $(x_{k+1}, y_{k+1}) = T_p(x_k, y_k)$ presented in the form

$$\begin{aligned} x_{k+1} &= x_k + 2\pi\omega(y_{k+1}) + \epsilon g(x_k, y_{k+1}) \\ y_{k+1} &= y_k + \epsilon f(x_k, y_{k+1}) \end{aligned} \tag{13}$$

with the perturbation functions $f(x_k, y_{k+1})$ and $g(x_k, y_{k+1})$ satisfying the area preserving condition: $\partial f/\partial x_k + \partial g/\partial y_{k+1} = 0$; $x \pmod{2\pi}$ and y are canonical variables.

The map (13), known as the perturbed twist map, describes the essential features of the Hamiltonian system (2) (see, e.g., [3, 30]). It has been extensively used in various areas to study Hamiltonian systems (2) by identifying the map variables x and y with the angle-action variables θ and I respectively, and the index k is identified as time instants t_k, i.e. $x_k = \theta(t_k)$, $y_k = I(t_k)$. The perturbed twist map (13) may be obtained from the symmetric map (9)–(11) as an approximate map for the intermediate variables $(\Theta_{k\pm0}, J_{k\pm0})$. For instance, in order to establish the map $(\Theta_{k+1-0}, J_{k+1-0}) = \hat{T}_p(\Theta_{k-0}, J_{k-0})$ we expand the generating functions $S_\pm(J_{k\pm0}, \theta_k)$ near the values $(J_{k+1-0}, \Theta_{k-0})$, and neglect terms of order ϵ. Then the perturbation functions $f(\Theta_{k-0}, J_{k+1-0})$ and $g(\Theta_{k-0}, J_{k+1-0})$ are determined by the generating function $G(\Theta_{k-0}, J_{k+1-0})$:

$$\begin{aligned} f(\Theta_{k-0}, J_{k+1-0}) &= -\frac{\partial G(\Theta_{k-0}, J_{k+1-0})}{\partial \Theta_{k-0}} \\ g(\Theta_{k-0}, J_{k+1-0}) &= \frac{\partial G(\Theta_{k-0}, J_{k+1-0})}{\partial J_{k-0}} \end{aligned} \tag{14}$$

where

$$G(J_{k+1-0}, \Theta_{k-0}) = S_+(J_{k+1-0}, \Theta_{k-0}) - S_-(J_{k+1-0}, \Theta_{k-0}). \tag{15}$$

Therefore, the variables in the perturbed twist mapping (13), do not coincide with the variables in Hamiltonian equations taken at the sections $t = t_k$, and they are related to those according to equations (9) and (11).

4. Generating function

The generating function $S(J, \vartheta)$ satisfies the equation:

$$\mathcal{H}\left(J, \vartheta + \epsilon\frac{\partial S}{\partial J}, t\right) = H\left(J + \epsilon\frac{\partial S}{\partial \vartheta}, \vartheta, t\right) + \epsilon\frac{\partial S}{\partial t}. \tag{16}$$

This equation may be solved using perturbation theory. The generating function $S \equiv S(J, \vartheta, t)$ will be sought as a series in powers of ϵ:

$$S(J, \vartheta, t) = S_1(J, \vartheta, t) + \epsilon S_2(J, \vartheta, t) + \cdots. \tag{17}$$

The new unperturbed $\mathcal{H}_0(J, \epsilon)$ and the perturbed $\mathcal{H}_1(J, \Theta, \epsilon)$ Hamiltonians in (4) are also sought as expansions:

$$\mathcal{H}_0(J, \epsilon) = \mathcal{H}_0^{(0)}(J) + \epsilon\mathcal{H}_0^{(1)}(J) + \cdots \tag{18}$$

$$\mathcal{H}_1(J, \vartheta, \epsilon) = \mathcal{H}_1^{(1)}(J, \vartheta) + \epsilon\mathcal{H}_1^{(2)}(J, \vartheta) + \cdots. \tag{19}$$

Expanding both sides of (16) in a series of powers of ϵ, and equating the terms with the same order in ϵ, one obtains

$$\mathcal{H}_0^{(0)}(J) = H_0(J) \tag{20}$$

$$\frac{\partial S_1}{\partial t} + \frac{\partial H_0}{\partial J}\cdot\frac{\partial S_1}{\partial \vartheta} = \mathcal{H}_0^{(1)}(J) + \mathcal{H}_1^{(1)}(J, \vartheta, t) - H_1(J, \vartheta, t) \tag{21}$$

$$\frac{\partial S_i}{\partial t} + \frac{\partial H_0}{\partial J}\cdot\frac{\partial S_i}{\partial \vartheta} = \mathcal{H}_0^{(i)}(J) + \mathcal{H}_1^{(i)}(J, \vartheta, t) - F_i(J, \vartheta, t) \qquad i \geqslant 2 \tag{22}$$

where the functions $F_i(J, \vartheta)$ are polynomials in $\partial S_1/\partial\vartheta, \ldots \partial S_{i-1}/\partial\vartheta$. Equations (21), (22) are valid in the time intervals $t_k < t < t_{k+1}$.

The terms $\mathcal{H}_0^{(i)}(J)$ ($i \geqslant 1$) describe the corrections to the unperturbed part of the Hamiltonian $H_0(J)$ and they do not depend on the angular variables ϑ and on time t. They may be found by the additional requirement that the averaging of equations (21) and (22) taken over angular variables ϑ are zero, i.e.

$$\begin{aligned} \mathcal{H}_0^{(1)}(J) &= \langle H_1(J, \vartheta, t)\rangle_\vartheta \\ \mathcal{H}_0^{(i)}(J) &= \langle F_i(J, \vartheta, t)\rangle_\vartheta . \end{aligned} \tag{23}$$

From equation (18) it follows that

$$\Omega(J, \epsilon) = \omega(J) + \epsilon \frac{\partial \mathcal{H}_0^{(1)}(J)}{\partial J} + \cdots .$$

The left-hand sides of equations (21) and (22) are total time derivatives taken along unperturbed trajectories $J(t)$ and $\vartheta(t)$ of the system (5), i.e.,

$$\frac{\mathrm{d}S_i}{\mathrm{d}t} = \frac{\partial S_i}{\partial t} + \frac{\partial H_0}{\partial J} \cdot \frac{\partial S_i}{\partial \vartheta}.$$

According to (4) the generating function $S_1(J, \theta, t)$ may be written as an integral

$$S_1(J, \theta, t) = -\int^t H_1(J, \vartheta(t'), t')\,\mathrm{d}t' + \mathcal{H}_0^{(1)}(J)t + C \tag{24}$$

where $\vartheta(t') = \vartheta(t) + \omega(J)(t' - t)$ and C is an integration constant. Then the solution of equation (21) in the time interval $t_k < t < t_{k+1}$ satisfying the condition $S_1(J, \vartheta, t) = 0$ at $t = t_k + \pi = 2\pi(k + 1/2)$ can be represented as

$$S_1(J, \vartheta, t) = \mathcal{H}_0^{(1)}(J)(t - t_k - \pi) - \int_{t_k+\pi}^t H_1(J, \vartheta(t'), t')\,\mathrm{d}t'. \tag{25}$$

The solution for $S_1(J, \theta, t)$ may also be found using a Fourier expansion of the perturbed old H_1 and new $\mathcal{H}_1$ Hamiltonians

$$H_1(J, \vartheta, t) = \sum_{m,n} H_{m,n}(J)\cos(\boldsymbol{m}\cdot\vartheta - nt + \varphi_{m,n}) \tag{26}$$

$$\mathcal{H}_1(J, \vartheta, t; 0) = \sum_{m} \mathcal{H}_m(J)\cos(\boldsymbol{m}\cdot\vartheta + \phi_m) \sum_{n=-\infty}^{\infty} \cos nt \tag{27}$$

where $\boldsymbol{m} = (m_1, \ldots, m_n)$, $\boldsymbol{m}\cdot\vartheta = m_1\vartheta_1 + \cdots + m_n\vartheta_n$, $\varphi_{m,n}$ and ϕ_m are the old and new phases, respectively. Direct integration of equation (21) with (26) and (27) using the summation formulae

$$\sum_{k=-\infty}^{\infty} \frac{1}{k + a} \begin{Bmatrix} \sin kx \\ \cos kx \end{Bmatrix} = \frac{\pi}{\sin \pi a} \begin{Bmatrix} \sin[x]a \\ \cos[x]a \end{Bmatrix}$$

where $[x] = (2s + 1)\pi - x$, $2\pi s < x < 2\pi(s + 1)$, $s = 0, \pm1, \pm2, \ldots$, gives

$$S_1(J, \vartheta, t) = \mathcal{H}_0^{(1)}(J)(t - t_k - \pi) + \sum_{m} S_m(J, \vartheta, t) \tag{28}$$

where

$$\begin{aligned} S_m(J, \vartheta, t) = \pi\mathcal{H}_m(J)&\frac{\sin(\boldsymbol{m}\cdot\vartheta + \boldsymbol{m}\cdot\omega(J)[t] + \phi_m)}{\sin(\pi\boldsymbol{m}\cdot\omega(J))} \\ &- \sum_n H_{m,n}(J)\frac{\sin(\boldsymbol{m}\cdot\vartheta - nt + \varphi_{m,n})}{\boldsymbol{m}\cdot\omega(J) - n}. \end{aligned} \tag{29}$$

Choosing the amplitudes $\mathcal{H}_m(J)$ and phases ϕ_m in order to satisfy the above condition $S_1(J, \vartheta, t) = 0$ at $t = 2\pi(k + 1/2)$ one obtains

$$S_m(J, \vartheta, t) = \sum_n H_{m,n}(J)\frac{\pi}{\alpha_{mn}(J)} \times\{\sin(\boldsymbol{m}\cdot\vartheta + \boldsymbol{m}\cdot\omega(J)[t] - n\pi + \varphi_{mn}) - \sin(\boldsymbol{m}\cdot\vartheta - nt + \varphi_{mn})\} \tag{30}$$

where $[t] = (2k + 1)\pi - t$, for $2\pi k < t < 2\pi(k + 1)$, and $\alpha_{mn}(J) = \pi(\boldsymbol{m}\cdot\omega(J) - n)$. The solution (30) may also be obtained from the integral (25) using the expansion (26). It is a discontinuous function of t at the values $t = t_k$. At the limit $t \to t_k \pm 0$ we have

$$S_\pm(J, \vartheta) = \mp\pi\mathcal{H}_0^{(1)}(J) + \sum_{m,n}\{S^{(s)}_{m,n}(J) \times \sin(\boldsymbol{m}\vartheta + \varphi_{mn}) \pm S^{(c)}_{m,n}(J)\cos(\boldsymbol{m}\vartheta + \varphi_{mn})\} \tag{31}$$

where

$$S^{(s)}_{mn}(J) = -\pi H_{mn}(J)\frac{1 - \cos\alpha_{mn}(J)}{\alpha_{mn}(J)}$$
$$S^{(c)}_{mn}(J) = \pi H_{mn}(J)\frac{\sin\alpha_{mn}(J)}{\alpha_{mn}(J)}. \tag{32}$$

In the equations (30)–(32) there are no divergent terms due to small denominators. Near the resonant values J_{mn}, i.e., $\boldsymbol{m}\cdot\omega(J_{mn}) = n$, the small terms $\alpha_{mn}(J)$ in the denominators of $S^{(s,c)}_{mn}$ cancel with the small numerators.

Consider a particular case of a single perturbation harmonics $n = \nu$ in (26). The map

$$(I_{k+1}, \vartheta_{k+1}) = \hat{T}^{(\nu)}(I_k, \vartheta_k) \tag{33}$$

corresponding to this case, is described by equations (9)–(11) with the variables (I, ϑ) taken at the time instants $t_k = k2\pi/\nu$. The corresponding generating function $S_\pm(J, \vartheta)$ is determined by

$$S^{(\nu)}_\pm(J, \vartheta) = \mp\frac{\pi}{\nu}\mathcal{H}_0^{(1)}(J) + \sum_m\{S^{(s)}_m(J)\sin(\boldsymbol{m}\vartheta + \varphi_{m\nu}) \pm S^{(c)}_m(J)\cos(\boldsymbol{m}\vartheta + \varphi_{m\nu})\} \tag{34}$$

where

$$S^{(s)}_m(J) = -\frac{\pi}{\nu}H_{m\nu}(J)\frac{1 - \cos\alpha_{m\nu}(J)}{\alpha_{m\nu}(J)}$$
$$S^{(c)}_m(J) = \frac{\pi}{\nu}H_{m\nu}(J)\frac{\sin\alpha_{m\nu}(J)}{\alpha_{m\nu}(J)} \tag{35}$$

with $\alpha_{m\nu}(J) = \pi(\omega(J)/\nu - 1)$.

5. Example. Magnetic field line dynamics in tokamaks

As an example we apply of the mapping method to study the chaotic dynamics of magnetic field lines in a tokamak ergodic divertor. It is well known that magnetic field lines satisfy the Hamiltonian system (2). We consider a simplified model for magnetic perturbation containing two toroidal modes n which does not take into account its radial dependence. A real model of magnetic perturbations in a toroidal system is studied in [31].

The corresponding Hamiltonian $H = H_0(I) + \epsilon H_1(\vartheta, t)$ may be represented by

$$H_0(I) = \ln I$$
$$\epsilon H_1(\vartheta, t) = \epsilon\sum_{n=1,2} c_n \sum_{m=-M+nm_0}^{M+nm_0} m^{-1} g_{mn}\cos(m\vartheta - nt) \tag{36}$$

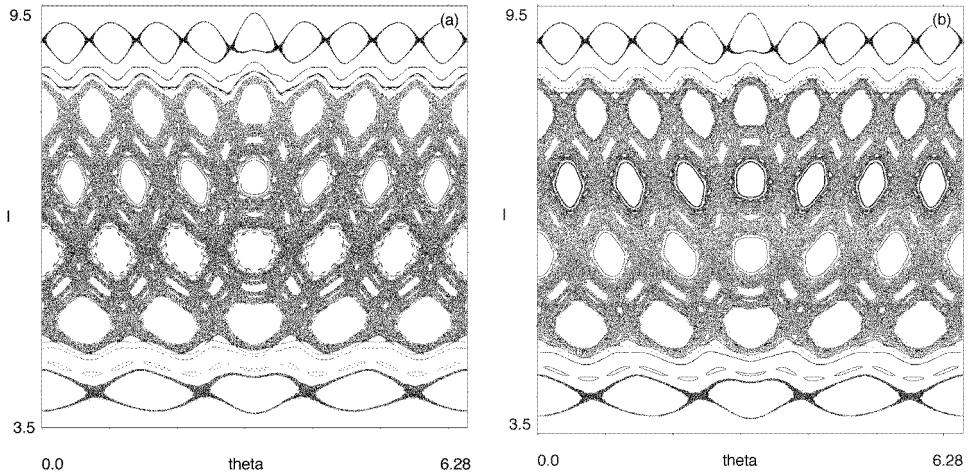

Figure 2. Poincaré sections obtained by the map (*a*) and by the integration of the equations of motion (*b*) for the Hamiltonian (36) with a single harmonics perturbation $n = 1$. The perturbation parameter $\epsilon = 0.03$, $m_0 = 6$, $N = 4$, and $M = 10$. (The 'theta' stands for θ.)

where

$$g_{mn} = (-1)^m \frac{\sin[(m - nm_0)\pi/N]}{\pi(m - nm_0)} \tag{37}$$

describes the spectrum of the magnetic perturbation. Here t is the toroidal angle, and ϑ is the poloidal angle. The perturbation H_1 is localized in a finite angular interval: $\pi(1-1/N) < \theta < \pi(1+1/N)$. The spectrum g_{mn} of each toroidal harmonics n is also localized near the central harmonics nm_0 with a width $\Delta m = 2N$. The coefficients $c_n (n = 1, 2)$ satisfy the condition $c_1 + c_2 = 1$, and they describe the relative contribution of each toroidal harmonics. The smallness parameter ϵ corresponds to the relative magnetic perturbation.

We consider the system (36) in a finite domain of action I, located near several resonances $m : n$ with the central ones being $m = m_0$, $n = 1$ and $m = 2m_0$, $n = 2$. The resonant actions, determined by the condition $\omega(I_{mn}) = n : m$, are $I_{mn} = m/n$. If the perturbation parameter ϵ exceeds a certain value ϵ_c these resonances start to overlap thereby forming a stochastic layer near the central resonant action $I_0 = m_0$.

For the numerical integration of the Hamiltonian equations (2), (36), (37) we have used the symplectic integration scheme with a constant integration step Δt. To plot Poincaré sections the integration step is taken equal to $\Delta t = 0.2$. To calculate a moment of mean square displacement $\langle(\Delta I(t))^2\rangle = \langle(I(t) - I_0)^2\rangle$ a smaller integration step $\Delta t = 0.01$ was chosen. ($\langle(\ldots)\rangle$ means averaging over the initial angle ϑ). Poincaré sections of the orbits are plotted in the (θ, I) plane.

First consider the case of a single $n = 1$ mode perturbation, i.e. $c_1 = 1$, $c_2 = 0$. The Poincaré sections obtained by the numerical integration and the map are shown in figure 2 ((a), map and (b), equation) for perturbation $\epsilon = 0.03$, the central harmonics number $m_0 = 6$, the effective width of spectrum $\Delta m = 2N = 8$, and the mode number $M = 10$. One can see from these figures that the map correctly reproduces the structure of the stochastic zone including the positions of the main and the secondary Kolmogorov–Arnold–Mozer (KAM) stability islands.

The moment of second-order displacement $\langle(\Delta I(t))^2\rangle$ is shown in figure 3 for the same parameters as in figure 1 and the initial action variable $I_0 = 5.7$: the curve 1 (thick) corresponds

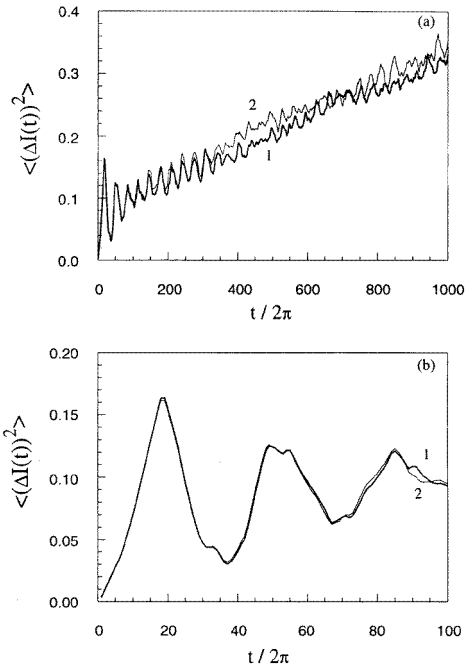

Figure 3. Comparison of the $\langle(\Delta I(t))^2\rangle$ versus t, calculated by the map (curve 1) and by the integration of equations of motion (curve 2). The parameters are the same as in figure 2.

to the map and the curve 2 (thin) corresponds to the equation. One can see from figure 2 that until $t < 200\pi$ there is no noticeable difference between the results of numerical integration and the map. For $t > 600\pi$ the deviation between them becomes noticeable. However, overall the map describes the behaviour of the second moment $\langle(\Delta I(t))^2\rangle$ sufficiently well for all time intervals shown in figure 3.

Let us turn to the perturbations with two-harmonics. This case may be directly studied by using the map (9)–(11) with the generating function (31) which includes both $n = 1$ and $n = 2$ harmonics. On the other hand, for this case one can establish a map obtained by successive coordinate transformations (3) applied separately to each harmonics n. Since the period $\Delta t = 2\pi$ of the $n = 1$ harmonics is twice as large as the period $\Delta t = \pi$ of $n = 2$ harmonics, the corresponding map $\hat{T}_s$ should be applied in a common period $\Delta t = 2\pi$:

$$(I_{k+2}, \vartheta_{k+2}) = \hat{T}_s(I_k, \vartheta_k) \tag{38}$$

where the variables (I_k, ϑ_k) are defined at the section $t = t_k = k\pi$.

In order to construct the map $\hat{T}_s$ we first apply the coordinate transformation $(I, \vartheta) \to (J, \Theta)$ (3), which transforms the perturbed Hamiltonian $H_1^{(1)}$ corresponding to $n = 1$ harmonics only without changing the $n = 2$ harmonics perturbation $H_1^{(2)}$:

$$\mathcal{H} = \mathcal{H}_0(J) + \epsilon\mathcal{H}_1^{(1)}(J, \Theta, t) + \epsilon H_1^{(2)}(J, \Theta, t) = H + \epsilon\frac{\partial S^{(1)}(J, \vartheta, t)}{\partial t} \tag{39}$$

where $\mathcal{H}_1^{(1)}$ is a new perturbed Hamiltonian (4) corresponding to the $n = 1$ harmonics, and $S^{(1)}(J, \vartheta, t)$ is its generating function. The second transformation $(J, \Theta) \to (\tilde{J}, \tilde{\Theta})$, given by the generating function $S^{(2)}(\tilde{J}, \Theta)$, transforms only the perturbed Hamiltonian $H_1^{(2)}$ corresponding the $n = 2$ harmonics:

$$\tilde{\mathcal{H}} = \tilde{\mathcal{H}}_0(\tilde{J}) + \epsilon\mathcal{H}_1^{(1)}(\tilde{J}, \tilde{\Theta}, t) + \epsilon\mathcal{H}_1^{(2)}(\tilde{J}, \tilde{\Theta}, t) = \mathcal{H} + \epsilon\frac{\partial S^{(2)}(\tilde{J}, \Theta, t)}{\partial t} \tag{40}$$

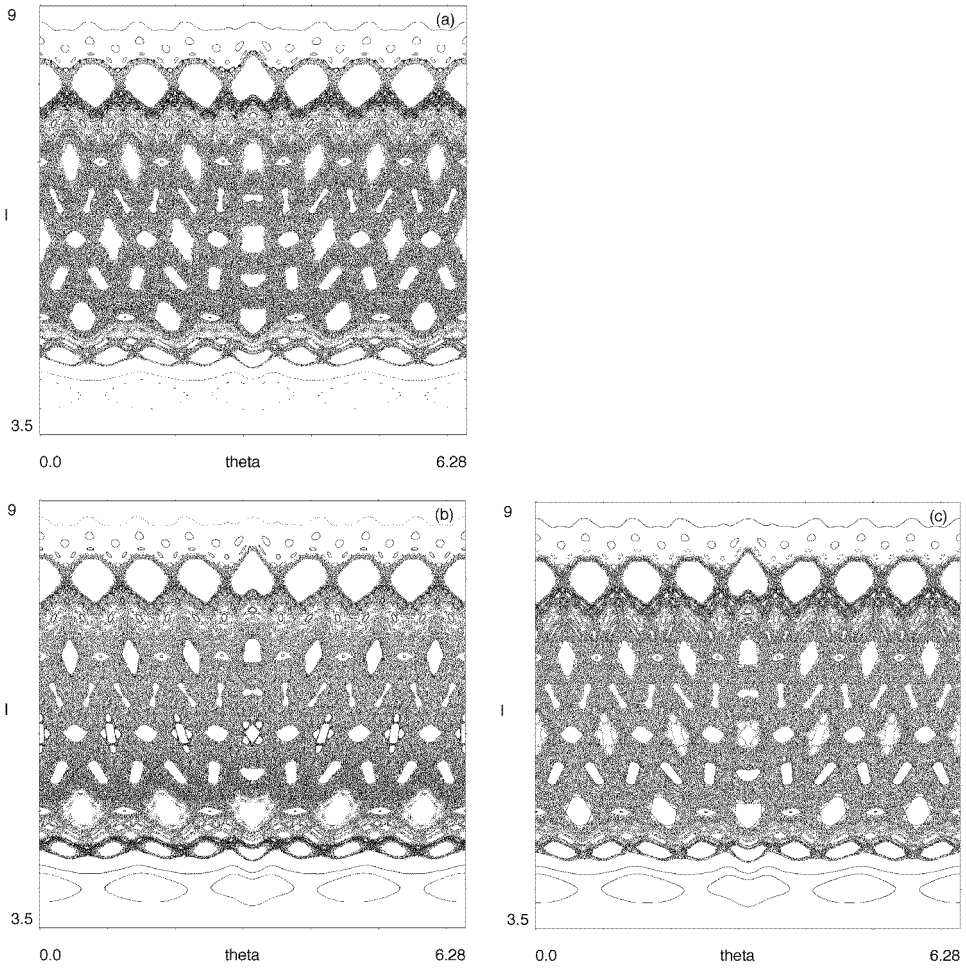

Figure 4. The same as in figure 2, but for the combination of the harmonics $n = 1$ and $n = 2$ ($c_1 = c_2 = 0.5$): (*a*) corresponds to the mapping with the generating function (31) including both harmonics $n = 1$ and $n = 2$, (*b*) corresponds to the mapping (38), (42) with (34), and (*c*) corresponds to the numerical integration.

where $\mathcal{H}_1^{(2)}$ is a new perturbed Hamiltonian of type (4) for $n = 2$ harmonics.

The evolution of the variables (J, Θ) is then described by the map $\hat{T}_s^{(2)}$ (33):

$$(J_{k+1}, \Theta_{k+1}) = \hat{T}_s^{(2)}(J_k, \Theta_k). \tag{41}$$

Since the period of $n = 1$ harmonics is twice as large as the period of $n = 2$ harmonics the map (38) may be written as

$$\hat{T}_s = \hat{T}_+^{(1)}(\hat{T}_s^{(2)})^2\hat{T}_-^{(1)} \tag{42}$$

where the operators $\hat{T}_\pm^{(1)}$, $\hat{T}^{(2)}$ are defined by equations (33), (9)–(11). In the first order of ϵ the corresponding generating functions $S_\pm^{(n)}$ are given by equation (34).

Poincaré sections for the two-harmonics perturbation with amplitudes $c_1 = c_2 = 0.5$ are presented in figures 4(*a*)–(*c*): (*a*) is obtained by the map with the generating functions (31) including both harmonics $n = 1$ and $n = 2$, and (*b*) is obtained by the map (38), (42)

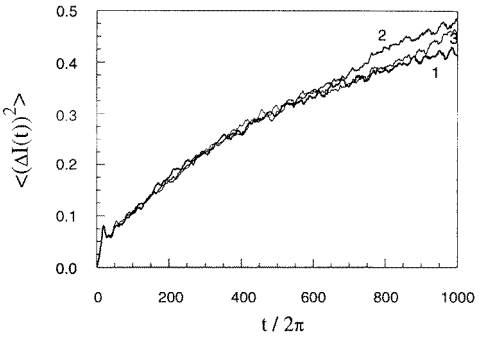

Figure 5. Dependence of the second moments $\langle(\Delta I(t))^2\rangle$ versus time corresponding to the Poincaré sections in figures 4(*a*)–(*c*). Curve 1 corresponds to the mapping with the generating function (31), curve 2 corresponds to the mapping (38), and curve 3 corresponds to the numerical integration.

with the generating functions (34). Figure 4(*c*) corresponds to the numerical integration of equations of motion. The values of the other parameters are the same as in figure 1. Poincaré sections in figures 4(*a*)–(*c*) are plotted by choosing identical initial conditions. At first glance both methods reproduce well the main features of the stochastic layer formed near the main harmonics $m_0 = 6$. A more careful comparison of figures 4(*a*)–(*c*) shows that the map (38), (42) more precisely reveals some fine details of the phase-space structure.

Figure 5 shows the dependence of the second moments $\langle(\Delta I(t))^2\rangle$ versus time corresponding to the Poincaré sections shown in figures 4(*a*)–(*c*). Curve 1 corresponds to the mapping (8) with the generating function (31), the curve 2 to the mapping (38), and curve 3 corresponds to the numerical integration with the integration step $\Delta t = 0.01$. At the initial stage $t < 80\pi$ results of the numerical integration are reproduced by both maps with a high precision.

One can conclude that the symmetric map sufficiently well describes the structure of Poincaré sections in the stochastic zone. It is also in good quantitative agreement with calculations of the moments of mean square displacement.

6. Standard Hamiltonian and standard map

The developed procedure also allows us to establish a map for the standard Hamiltonian (43):

$$H = \frac{I^2}{2} + \frac{K}{4\pi^2}\sum_{n=-M}^{M}\cos(\vartheta - nt). \tag{43}$$

It is usually supposed that for $M \to \infty$ the Hamiltonian (43) gives the Chirikov–Taylor map [3, 7]:

$$y_{k+1} = y_k + K\sin\vartheta_k \qquad \vartheta_{k+1} = \vartheta_k + y_{k+1} \tag{44}$$

whereby the variable y is identified by $2\pi I$. This map is a particular form of the perturbed twist map (13) and it is well known as a standard map. It has been extensively studied during the past two decades as one of the basic models in chaos theory and has been used in a variety physical problems, for instance to study particle–wave interaction, the magnetic field line dynamics in magnetic confinement devices (see [8–10]). Below we derive a symmetric symplectic map corresponding to the standard Hamiltonian (43) and study its relation to the standard map (44).

One should note that a direct numerical integration of the standard Hamiltonian (43) encounters difficulties for large numbers of modes $M \gg 1$. This is because the perturbation becomes fast oscillating and localized near the periodic time instants $t_k = 2\pi k$. It makes the numerical integration of this system unreliable [32].

Consider the case of a large, but a finite number of modes $M \gg 1$. Then the Hamiltonian (43) is continuous, and therefore one can apply the procedure of canonical transformations presented in section 3. The perturbation parameter ϵ in this case is equal to $\epsilon = K/4\pi^2$. According to (43), (31) and (32), the generating function $S_\pm(J, \vartheta)$ is in the first order of perturbation theory:

$$S_\pm(J, \vartheta) = S^{(s)}(J) \sin \vartheta \pm S^{(c)}(J) \cos \vartheta \tag{45}$$

where

$$S^{(c)}(J) = \sin(\pi\omega(J)) \sum_{n=-M}^{n=M} \frac{(-1)^n}{\omega(J) - n}$$

$$S^{(s)}(J) = -\sum_{n=-M}^{n=M} \frac{1 - (-1)^n \cos(\pi\omega(J))}{\omega(J) - n}$$

and $\omega(J) = J$. For large $M \gg 1$, we have $S^{(c)}(J) \approx \pi$, $S^{(s)}(J) \approx 0$, and therefore

$$\epsilon S_\pm(J, \vartheta) \approx \pm(K/4\pi) \cos \vartheta. \tag{46}$$

The symmetric symplectic map (8) takes the form

$$\begin{aligned} P_{k+0} &= p_k + (K/2) \sin \vartheta_k \\ P_{k+1-0} &= P_{k+0} \qquad \vartheta_{k+1} = \vartheta_k + P_{k+1-0} \\ p_{k+1} &= P_{k+1-0} + (K/2) \sin \vartheta_{k+1} \end{aligned} \tag{47}$$

where $p_k = 2\pi I_k$, $P_{k\pm0} = 2\pi J_{k\pm0}$. From (47) one can obtain the standard map (44) identifying the variable y_k with P_{k-0}.

The map (47) is also valid for large values of the perturbation parameter K. Indeed for a sufficiently large mode number M the perturbed part of the Hamiltonian (43) may be approximately replaced by a sum of $\delta-$ functions. Then integration of the equations of motion gives the standard map (44) for the variables ϑ_k and P_{k-0}. Since the standard map is a particular case of the perturbed twist map (13) with the generating function $G(J, \vartheta) = (K/2\pi) \cos \vartheta$, from (12) and (15) there follows (46). Further we will call the map (47) a symmetric standard map.

We have compared the time-dependence of $\langle(\Delta I(t))^2\rangle$ obtained by the symmetric map and by numerical integration presented in figure 6: (*a*) corresponds to the mode number $M = 5$, and (*b*) corresponds to $M = 10$, respectively. Curve 1 corresponds to the symmetric map and curve 2 corresponds to the numerical integration (the integration step Δt is 0.01). The perturbation parameter $K = 1.5$. As seen from figure 6 for $M = 5$ and $M = 10$ the symmetric map reproduces well the results of numerical integration.

For a large mode number M the symmetric map may be replaced by the symmetric standard map (47) that is shown in figure 7 for $M = 20$: curve 1 corresponds to the symmetric map, curve 2 corresponds to the symmetric standard map (47), curve 3 describes the numerical integration, and curve 4 corresponds to the standard map (44). For $M = 20$ the difference between curves 1 and 3 increases with time because of uncertainty of the numerical integration for this case.

However, one can see that for all time intervals the symmetric map is in good agreement with the symmetric standard map (curve 3). At the same time the standard map gives a very noisy curve (curve 4), which is far from the results of the symmetric map and the symmetric standard map.

Therefore the symmetric map (8)–(11) and the symmetric standard map (47) describe more correctly the evolution of the standard Hamiltonian than the standard map (44).

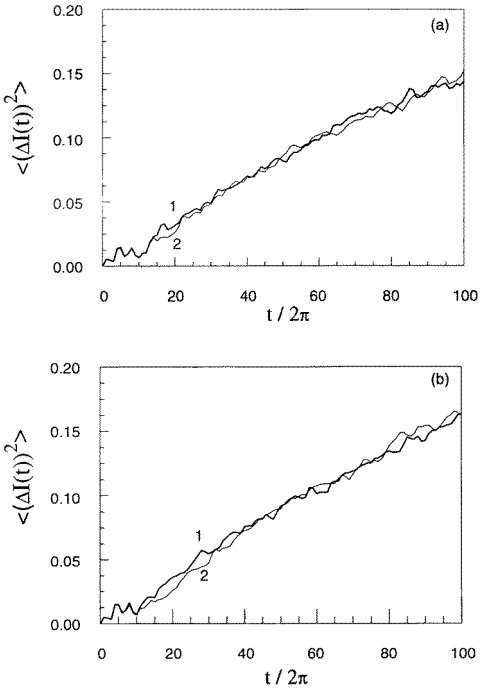

Figure 6. Second moments $\langle(\Delta I(t))^2\rangle$ versus t for the standard Hamiltonian (43): (*a*) corresponds to the mode number $M = 5$, and (*b*) corresponds to $M = 10$, respectively. Curve 1 corresponds to the symmetric map and curve 2 corresponds to the numerical integration with the integration step $\Delta t = 0.01$. The perturbation parameter $K = 1.5$.

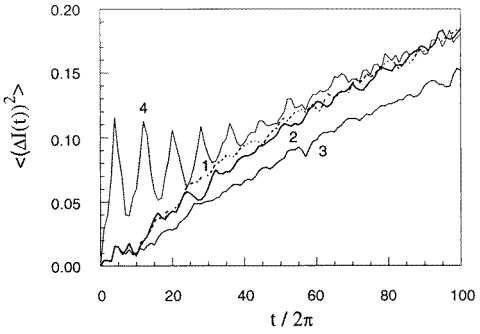

Figure 7. The same as in figure 6, but for $M = 20$. Curve 1 corresponds to the symmetric map, curve 2 corresponds to the symmetric standard map (47), curve 3 describes the numerical integration, and curve 4 corresponds to standard map (44). The perturbation parameter K is the same as figure 6.

7. Poincaré maps at arbitrary phase-space sections

The procedure described in section 2 may also be applied to obtain a Poincaré map at an arbitrary cross-section of the phase space. Consider the definite section where $\vartheta_N \pmod{2\pi} = \chi = \text{const}$. We should reformulate the Hamiltonian equations introducing ϑ_N as an independent 'time' variable and the corresponding action I_N as Hamiltonian. The real time variable t and the Hamiltonian H will be considered as additional angle and action variables respectively. Inverting the Hamiltonian $H = H_0(I) + \epsilon H_1(I, \vartheta, t)$ with respect to I_N Hamiltonian equations with the independent variable ϑ_N may be written as

$$\frac{\mathrm{d}\overline{\vartheta}_i}{\mathrm{d}\vartheta_N} = \frac{\partial F}{\partial \overline{I}_i} \qquad \frac{\mathrm{d}\overline{I}_i}{\mathrm{d}\vartheta_N} = -\frac{\partial F}{\partial \overline{\vartheta}_i} \qquad i = 1, \ldots, N \tag{48}$$

where F is a corresponding Hamiltonian function:

$$F \equiv I_N = F_0(\overline{I}) + \epsilon F_1(\overline{I}, \overline{\vartheta}, \vartheta_N; \epsilon) \tag{49}$$

written as a sum of unperturbed F_0 and perturbed F_1 parts. In (48) $\overline{I} = (I_1, \ldots, I_{N-1}, H)$, $\overline{\vartheta} = (\vartheta_1, \ldots, \vartheta_{N-1}, t)$, The unperturbed frequencies of the system (48) are

$$f_i(\overline{I}) = \frac{\partial F_0(\overline{I})}{\partial \overline{I}_i} = \frac{\partial I_N}{\partial H}\frac{\partial H}{\partial \overline{I}_i} = \frac{\omega_i(\overline{I})}{\omega_N(\overline{I})} \qquad i = 1, \ldots, N$$

where $\omega_i(\overline{I}) = \partial H_0(I)/\partial I_i$, $(i = 1, \ldots, N)$ are frequencies of original Hamiltonian $H_0(I)$. Particularly, we have $f_N(\overline{I}) = 1/\omega_N(\overline{I})$.

A Poincaré map at the section $\vartheta_N \pmod{2\pi} = \chi$ may be constructed by a canonical transformation $(\overline{I}, \overline{\vartheta}) \to (\overline{J}, \overline{\Theta})$ of type (3) with the generating function $F = \overline{J}\overline{\vartheta} + \epsilon S(\overline{J}, \overline{\vartheta}, \vartheta_N)$. Here $\overline{J} = (J_1, \ldots, J_{N-1}, \mathcal{H})$, $\overline{\Theta} = (\Theta_1, \ldots, \Theta_{N-1}, T)$. It transforms the Hamiltonian (49) into a new one:

$$\begin{aligned}
&\mathcal{F} = \mathcal{F}_0(\overline{J}, \epsilon) + \epsilon\mathcal{F}_1(\overline{J}, \overline{\Theta}, \vartheta_N, \epsilon) \\
&\mathcal{F}_1(\overline{J}, \overline{\Theta}, \vartheta_N, \epsilon) = \mathcal{F}_1(\overline{J}, \overline{\Theta}, \epsilon) \sum_{n=-\infty}^{\infty} \cos n(\vartheta_N - \chi) \\
&\qquad = 2\pi\mathcal{F}_1(\overline{J}, \overline{\Theta}, \epsilon) \sum_{k=-\infty}^{\infty} \delta(\vartheta_N - 2\pi k - \chi).
\end{aligned} \tag{50}$$

Using a procedure described in section 2 one can establish a return map (Poincaré map) at the section $\vartheta_N (\mathrm{mod} 2\pi) = \chi$, i.e.

$$(\overline{I}_{k+1}, \overline{\vartheta}_{k+1}) = \hat{T}_s(\overline{I}_k, \overline{\vartheta}_k) \tag{51}$$

where $(\overline{I}_k, \overline{\vartheta}_k) = (\overline{I}(\vartheta_{Nk}), \overline{\vartheta}(\vartheta_{Nk}))$, $\vartheta_{Nk} = 2\pi k + \chi$, and $(\overline{I}(\vartheta_N), \overline{\vartheta}(\vartheta_N))$ is a trajectory of the perturbed system (48). The map (51) has a form similar to (9)–(11) with the generating functions $S_\pm(\overline{J}, \overline{\vartheta}) = \lim_{\vartheta_N \to \vartheta_{Nk} \pm 0} S(\overline{J}, \overline{\vartheta}, \vartheta_N)$, and the frequencies $\Omega(\overline{J}, \epsilon) = \partial\mathcal{F}_0(\overline{J}, \epsilon)/\partial\overline{J}$.

In the first order of perturbation theory we have

$$\begin{aligned}
&F_1(\overline{J}, \vartheta_N, \epsilon) = \frac{\partial F_0(\overline{J})}{\partial H}\overline{H}_1(\overline{J}, \vartheta, t) \\
&\Omega_i(\overline{J}, \epsilon) = f_i(\overline{J}) + \epsilon\frac{\partial\mathcal{F}_0^{(1)}(\overline{J})}{\partial J_i} \qquad i = 1, \ldots, N
\end{aligned} \tag{52}$$

where $\mathcal{F}_0^{(1)}(\overline{J}) = \langle F_1(\overline{J}, \overline{\vartheta}, \vartheta_N)\rangle_\vartheta$, and $\overline{H}_1(\overline{J}, \vartheta, t) \equiv H_1(J_1, \ldots, J_{N-1}, J_N(\overline{J}), \vartheta, t)$.

Similarly to (25), one can obtain the following expression for the generating function:

$$S_1(\overline{J}, \overline{\vartheta}, \vartheta_N) = \mathcal{F}_0^{(1)}(\overline{J})(\vartheta_N - \vartheta_{Nk} - \pi) - \int_{\vartheta_{Nk}+\pi}^{\vartheta_N} F_1(\overline{J}, \overline{\vartheta}(\vartheta'_N), \vartheta'_N)\,\mathrm{d}\vartheta'_N \tag{53}$$

where the integral is taken along unperturbed trajectories $\overline{\vartheta}(\vartheta'_N) = \overline{\vartheta}(\vartheta_N) + f(\overline{J})(\vartheta'_N - \vartheta_N)$. Using (52), equation (53) may be rewritten in terms of the unperturbed trajectory $\vartheta(t') = \vartheta(t) + \omega(\overline{J})(t' - t)$ of the original Hamiltonian $H_0(I)$:

$$S_1(\overline{J}, \vartheta, t) = \mathcal{H}_0^{(1)}(\overline{J})(t - t_k - \pi/\omega_N(\overline{J})) - \int_{t_k+\pi/\omega_N(\overline{J})}^{t} \overline{H}_1(\overline{J}, \vartheta(t'), t')\,\mathrm{d}t'. \tag{54}$$

Here t_k is a time instant when the trajectory $\vartheta(t)$ crosses the section $\vartheta_N \pmod{2\pi} = \chi$, i.e. $\vartheta_N(t_k) \pmod{2\pi} = \chi$. From (54) one obtains the generating function $S_\pm(\overline{J}, \overline{\vartheta})$ for the map (51)

$$S_\pm(\overline{J}, \overline{\vartheta}) = \pm\pi\mathcal{H}_0^{(1)}(\overline{J})/\omega_N(\overline{J}) - \int_{t_k \pm \pi/\omega_N(\overline{J})}^{t_k} \overline{H}_1(\overline{J}, \vartheta(t'), t')\,\mathrm{d}t'. \tag{55}$$

The map (51) constructed by the three intermediate maps (9)–(11) with the generating function (55) defining a Poincaré map at the section $\vartheta_N \pmod{2\pi} = \chi$. This map is valid for explicitly time-dependent Hamiltonian systems, as well as for autonomous systems. In the latter case the Hamiltonian H is an integral of motion.

Consider, for example, the one-degree-of-freedom Hamiltonian system with a small time-periodic perturbation

$$H = H_0(I) + \epsilon H_1(I, \vartheta, t) \qquad H_1(I, \vartheta, t) = H_1(I, \vartheta, t + 2\pi/\nu) \tag{56}$$

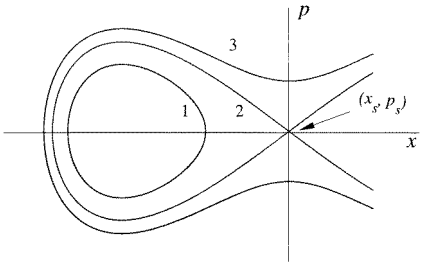

Figure 8. Schematic view of the phase space of a Hamiltonian system with one hyperbolic fixed point at $(x = x_s, p = p_s)$. Curve 1 describes a trapped motion, curve 2 corresponds to the separatrix, curve 3 describes untrapped motion.

where ν is a perturbation frequency. Suppose for simplicity that $\mathcal{H}_0^{(1)}(\overline{J}) = 0$. According to (9)–(11) and (55) the Poincaré map $(t_{k+1}, H_{k+1}) = \hat{T}_s(t_k, H_k)$ of the time and energy variables onto the section $\vartheta \pmod{2\pi} = \chi$ has a form

$$\mathcal{H}_{k+0} = H_k - \epsilon \frac{\partial S_+(\mathcal{H}_{k+0}, t_k)}{\partial t_k} \qquad T_{k+0} = t_k + \epsilon \frac{\partial S_+(\mathcal{H}_{k+0}, t_k)}{\partial \mathcal{H}_{k+0}} \tag{57}$$

$$\mathcal{H}_{k+1-0} = \mathcal{H}_{k+0} \qquad T_{k+1-0} = T_{k+0} + 2\pi/\omega(\mathcal{H}_{k+1-0}) \tag{58}$$

$$H_{k+1} = \mathcal{H}_{k+1-0} + \epsilon \frac{\partial S_-(\mathcal{H}_{k+1-0}, t_{k+1})}{\partial t_{k+1}} \qquad t_{k+0} = T_k - \epsilon \frac{\partial S_-(\mathcal{H}_{k+1-0}, t_{k+1})}{\partial \mathcal{H}_{k+1-0}} \tag{59}$$

where

$$S_\pm(\mathcal{H}, t_k) = -\int_{t_k \pm \pi/\omega(\mathcal{H})}^{t_k} H_1(I(\mathcal{H}), \vartheta(t'), t')\, \mathrm{d}t'. \tag{60}$$

$\omega(H) = \mathrm{d}H_0/\mathrm{d}I$ and $I(H)$ is the inverse of the relation $H = H_0(I)$.

8. Maps near the separatrix

A separatrix is a phase-space curve separating regions with different types of motion. Any small periodic perturbation destroys the separatrix and creates a stochastic layer near the unperturbed separatrix. The study of motion near the separatrix is generic for a nonlinear Hamiltonian system. It has been studied over a long time because of its importance to many physical applications [7, 8, 16, 20, 33]. The first attempt to construct an area-preserving map near the separatrix map was made in [33]. The simplest map near the separatrix was proposed in [7] in terms of time and energy variables, and was called a separatrix (whisker) map. The geometric interpretation of the separatrix map was given later in [34]. The separatrix map introduced in [7, 8, 16, 20, 33] has a specific feature: it is a return map of time and energy variables defined at different sections. In [12, 13], generalized separatrix maps were introduced for time and energy variables defined at the same sections.

Below we present a rigorous derivation of the maps near the separatrix. For the sake of simplicity consider a one-degree-of-freedom Hamiltonian system $H_0(x, p)$ with (x, p) being the canonical coordinate and momentum. Suppose that the system has one hyperbolic fixed point at $(x = x_s, p = p_s)$. Figure 8 shows a schematic view of the phase space: Curve 1 describes a trapped motion, curve 3 corresponds to an untrapped one. Curve 2 describes the separatrix. Near the hyperbolic fixed point the unperturbed Hamiltonian may be expanded in a power series of $x - x_s$ and $p - p_s$:

$$H_0(x, p) = H_s - \frac{\alpha^2}{2}(x - x_s)^2 + \frac{\beta^2}{2}(p - p_s)^2 + O(\Delta x^3, \Delta p^3, \Delta x^2 \Delta p, \Delta x \Delta p^2) \tag{61}$$

where $H_s = H_0(x_s, p_s)$, $\Delta x = x - x_s$, $\Delta p = p - p_s$. Furthermore, without loss of generality one can put $H_s = 0$.

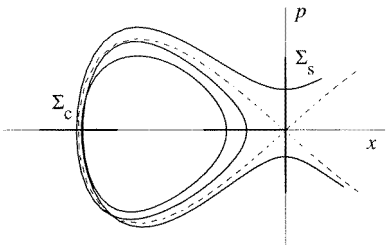

Figure 9. Definition of the sections Σ_c and Σ_s on the phase space (x, p) of a Hamiltonian system.

For the trapped unperturbed motion ($H < 0$) one can introduce action-angle variables: (I, ϑ):

$$I = \frac{1}{2\pi}\oint_{C_i} p(x; H)\mathrm{d}x \qquad \vartheta = \frac{\partial}{\partial I}\int^{x} p(x'; H)\mathrm{d}x' \tag{62}$$

where C_i is a closed contour along the phase-space curve i (i=1, 2) of constant $H = H_0(x, p)$. We will further introduce action-angle variables (I, ϑ) for the untrapped motion ($H > 0$) similar to (62) and it is taken along the segment of the contour C_3 located on the left side of the (x, p)-plane, i.e. $x < x_s$. In this way the action variable I becomes a continuous function of energy H at the separatrix $H = H_s$.

The period of motion $T(H) = 2\pi/\omega(H)$ near the separatrix goes to infinity, i.e., $T(H) \to \infty$ (or $\omega(H) \to 0$) for $H \to 0$. If the saddle point (x_s, p_s) lies in a finite domain of the phase space the asymptotics of $T(H)$ is universal, i.e.

$$T(H) = \frac{1}{\gamma}\ln\frac{Q}{|H|} + O(H) \qquad \text{for} \quad H \to \pm 0 \tag{63}$$

where γ is determined by the expansion coefficients α and β in (61): $\gamma = \alpha\beta$, and the parameter Q depends on the systems' properties.

Suppose that the system is subjected to a small time-periodic perturbation with a frequency ν. In the action-angle variables the Hamiltonian may be represented by equation (56). The perturbation destroys the separatrix and the motion near the separatrix becomes chaotic as it is shown in figure 9): a chaotic trajectory (a solid curve) wobbles around the unperturbed separatrix (dotted curve).

A chaotic motion near the separatrix may be conveniently described by a map of time (t) and energy (H) variables at certain sections of the phase-space (x, p). One can consider the sections Σ_c and Σ_s, shown in figure 9. The section Σ_c consists of segments of the x axis located near the farthest crossing points of the unperturbed separatrix with the x axis. The section Σ_s is located near the hyperbolic saddle point (x_s, p_s) and consists of two segments of the x and p axes with the centre at (x_s, p_s) which are perpendicular to each other.

To construct a map one could use the method presented in section 7. However, this method fails near the separatrix where the motion frequency behaves like $\omega(H) = \mathrm{d}H_0/\mathrm{d}I \to 0$ (or $\mathrm{d}I/\mathrm{d}H_0 \to \infty$). This singularity does not allow us to invert the Hamiltonian $H(I, \vartheta, t)$ in respect to the action variable I near the separatrix and to represent it in the form (49). Below we present another method to construct a Poincaré map near the separatrix.

Let t_k and H_k be a time instant and an energy at the kth crossing point of the orbit with the section Σ_c (or Σ_s). We will construct a return map

$$(t_{k+1}, H_{k+1}) = \hat{T}_s(t_k, H_k). \tag{64}$$

A change of the angular variable ϑ in one step of the map (64) is equal to $\Delta\vartheta \equiv \vartheta_{k+1} - \vartheta_k = 2\pi$.

Notice that a one-and-a-half-degree-of-freedom Hamiltonian system $H = H_0(I) + \epsilon H_1(I, \vartheta, t)$ may be replaced by a two-degree-of-freedom Hamiltonian

$$\overline{H}(I, H, \vartheta, t) = H_0(I) - H + \epsilon H_1(I(H), \vartheta, t) = 0 \tag{65}$$

in the extended phase space (I, H, ϑ, t). Let τ be an independent time variable $\tau = t$. In (65) the perturbation H_1 is chosen as a function of an energy H. Suppose that the trajectory crosses the Σ_c (or Σ_s) at $\tau = \tau_k$.

We apply a canonical coordinate transformation $(I, H, \vartheta, t) \to (J, \mathcal{H}, \Theta, T)$ (3) to (65), which eliminates the perturbation in the time intervals $\tau_k < \tau < \tau_{k+1}$, i.e. $\overline{H} \to \overline{\mathcal{H}}$:

$$\overline{\mathcal{H}}(J, \mathcal{H}, \Theta, T, \tau) = \mathcal{H}_0(J, \epsilon) - \mathcal{H} + 2\pi\epsilon\mathcal{H}_1(\mathcal{H}, \Theta, T, \epsilon) \sum_{k=-\infty}^{\infty} \delta(\tau - \tau_k). \tag{66}$$

The generating function associated with the transformation is $F = J\vartheta - \mathcal{H}t + \epsilon S(\mathcal{H}, J\vartheta, t)$. Because the perturbation H_1 in (65) is independent of the action I, the function $S(\mathcal{H}, J, \vartheta, t)$ also does not depend on J in the first order of perturbation theory, and therefore the new angle Θ coincides with the old angle ϑ. Suppose that $\mathcal{H}_0^{(1)}(\mathcal{H}) = 0$.

The map $(I_k, H_k, \vartheta_k, t_k) \to (I_{k+1}, H_{k+1}, \vartheta_{k+1}, t_{k+1})$ is constructed as in section 2. In the first order of ϵ a part of the map containing the action-angle variables (I, ϑ) is

$$\begin{aligned} J_{k+0} &= I_k - \frac{\partial S_+}{\partial \vartheta_k} \\ \vartheta_{k+1} &= \vartheta_k + \omega(J_{k+0}, \mathcal{H}_{k+0})(\tau_{k+1} - \tau_k) \\ I_{k+1} &= J_{k+0} + \frac{\partial S_-}{\partial \vartheta_{k+1}}. \end{aligned} \tag{67}$$

A Poincaré recurrence time $\Delta\tau = \tau_{k+1} - \tau_k$ is determined by the above-mentioned fact that $\Delta\vartheta = 2\pi$, i.e. $\Delta\tau = 2\pi/\omega(\mathcal{H}, \epsilon)$.

Then the map (64) can be represented by (57)–(59) with the corresponding generating functions (60).

The mapping at the sections Σ_c. Suppose that the perturbation contains single harmonics. The perturbed Hamiltonian $H_1(I(H), \vartheta(t), t)$ in (55) taken on the unperturbed trajectory may be represented by

$$\epsilon H_1(I(H), \vartheta(t), t) = V(\mathcal{H}, t - t_k)\cos(\nu t + \chi) \tag{68}$$

where t_k is the time instant when the trajectory crosses the section Σ_c, and χ is a phase of the perturbation. Then the generating functions $S_\pm(\mathcal{H}, t_k)$ take the from

$$S_\pm(\mathcal{H}, t_k) = K^{(\pm)}(\mathcal{H})\cos(\nu t_k + \chi) - L^{(\pm)}(\mathcal{H})\sin(\nu t_k + \chi) \tag{69}$$

where

$$K^{(\pm)}(\mathcal{H}) = \pm \int_0^{\pi/\omega(\mathcal{H})} V(\mathcal{H}, \pm\tau)\cos(\nu\tau)\mathrm{d}\tau \tag{70}$$

$$L^{(\pm)}(\mathcal{H}) = \int_0^{\pi/\omega(\mathcal{H})} V(\mathcal{H}, \pm\tau)\sin(\nu\tau)\mathrm{d}\tau. \tag{71}$$

The mapping (64), (57)–(59) with the generating function (69) is a return map of variables (t, H) at the section Σ_c (see figure 9).

The mapping (64), (57)–(59) can be simplified if the width of the stochastic layer near the separatrix is rather small. Indeed, in this case due to a weak dependence of the integrals (70) and (71) on the energy $\mathcal{H}$ and due to the fact that the stochastic layer is located in a small vicinity of the unperturbed separatrix one can neglect the dependencies of the quantities

$K^{(\pm)}(\mathcal{H})$ and $L^{(\pm)}(\mathcal{H})$ on $\mathcal{H}$ and instead take their values at $\mathcal{H} = 0$. Taking into account that $\omega(H) \to 0$ for $H \to 0$ we have the following simplified map near the separatrix:

$$\begin{aligned} \mathcal{H}_{k+0} &= H_k + \epsilon\nu\{K^{(+)}\sin(\varphi_k + \chi) + L^{(+)}\cos(\varphi_k + \chi)\} \\ \mathcal{H}_{k+1-0} &= \mathcal{H}_{k+0}\varphi_{k+1} = \varphi_k + 2\pi\nu/\omega(\mathcal{H}_{k+1-0}) \\ H_{k+1} &= \mathcal{H}_{k+1-0} + \epsilon\nu\{K^{(-)}\sin(\varphi_{k+1} + \chi) + L^{(-)}\cos(\varphi_{k+1} + \chi)\} \end{aligned} \tag{72}$$

where $\varphi_k = \nu t_k$, and

$$K^{(\pm)} \equiv K^{(\pm)}(0) = \pm\int_0^\infty V(0, \pm\tau)\cos(\nu\tau)\mathrm{d}\tau \tag{73}$$

$$L^{(\pm)} \equiv L^{(\pm)}(0) = \int_0^\infty V(0, \pm\tau)\sin(\nu\tau)\mathrm{d}\tau. \tag{74}$$

The integrals in (73) and (74) are taken along the unperturbed separatrix. One should notice that as the generating function $S(\mathcal{H}, t, \vartheta) = 0$ at the section $\vartheta = 2\pi k + \pi$, i.e., at the section Σ_s (see figure 9) the intermediate variable $\mathcal{H}_{k\pm0}$ is equal to the energy at Σ_s.

The map (72) may be written in terms of the variables $(\mathcal{H}_{k+0}, t_k)$ defined at the sections Σ_s and Σ_c, respectively:

$$\begin{aligned} \mathcal{H}_{k+1-0} &= \mathcal{H}_{k-0} + \epsilon\nu\{K\sin(\varphi_k + \chi) + L\cos(\varphi_k + \chi)\} \\ \varphi_{k+1} &= \varphi_k + 2\pi\nu/\omega(\mathcal{H}_{k+1-0}) \end{aligned} \tag{75}$$

where

$$K = \int_{-\infty}^\infty V(0, \tau)\cos(\nu\tau)\mathrm{d}\tau \qquad L = \int_{-\infty}^\infty V(0, \tau)\sin(\nu\tau)\mathrm{d}\tau. \tag{76}$$

The second term on the right-hand side of the separatrix mapping (75) is the Melnikov integral [35]. Equations (75) are a conventional form of the separatrix map.

For systems with a hyperbolic fixed point the maps (72) and (75) are invariant with respect to the transformation of the perturbation parameter ϵ and the energy H:

$$\epsilon \to \lambda\epsilon \qquad H \to \lambda H \qquad \lambda = \exp(2\pi\gamma/\nu) \tag{77}$$

where λ is a rescaling parameter determined by the perturbation frequency ν and the parameter $\gamma = \alpha\beta$. The latter is a product of the expansion coefficients α and β in (61). This property simply results from the universal logarithmic behaviour (63) of the motion frequency $\omega(H)$ near the separatrix, and was first established in [36, 37].

The mapping at the section Σ_s. The trajectories in the stochastic layer, formed in the vicinity of the unperturbed separatrix, spend most of their time near the saddle points. Therefore, the dynamics of the system and its statistical properties are mainly determined by the structure of the stochastic layer near these points. Therefore, it is important to establish a mapping describing the motion near the saddle point. In such a map both variables (H, t) should be defined at the section Σ_s (see figure 5). This may be obtained from the separatrix map (75), shifting the time variable t_k from the section Σ_c to the section Σ_s. Since t_k at the section Σ_c is shifted by half a period of the unperturbed motion $\pi/\omega(H)$ from t_k at the section Σ_s (see figure 9) and because $\mathcal{H}$ coincides with H taken at the section Σ_c, we have the following map:

$$\begin{aligned} H_{k+1} &= H_k + \epsilon\nu\left\{K\sin\left(\varphi_k + \frac{\pi\nu}{\omega(H_k)} + \chi\right) + L\cos\left(\varphi_k + \frac{\pi\nu}{\omega(H_k)} + \chi\right)\right\} \\ \varphi_{k+1} &= \varphi_k + \frac{\pi\nu}{\omega(H_k)} + \frac{\pi\nu}{\omega(H_{k+1})} \end{aligned} \tag{78}$$

where both variables (H, t) are defined at the section Σ_s located near the hyperbolic fixed point (x_s, p_s). The mapping (78) was first introduced in [12, 13], and was called a shifted separatrix map.

Unlike the separatrix map (75), the map (78) is invariant with respect to the following transformation of a perturbation parameter ϵ, the energy H and the perturbation phase χ:

$$\epsilon \to \lambda\epsilon \qquad H \to \lambda H \qquad \chi \to \chi + \pi. \tag{79}$$

This describes the important, nontrivial rescaling property of the motion near the hyperbolic fixed point, which has recently been established in [36, 37] by numerical simulations, and also in [12, 13] by introducing the shifted separatrix mappings. An analytical proof of this property for some classes of perturbation was given in [38]. This property describes the fact that the transformations (79) of the amplitude, ϵ, and phase, χ, of the time-periodic perturbation preserve the topology of the phase space of the canonical variables (x, p) near the hyperbolic saddle point, with the rescaling law: $x \to \lambda^{1/2}x$, $p \to \lambda^{1/2}p$ (see, e.g., [38]).

Applications of the separatrix mappings to the problems of diffusion and transport has been considered in several publications [16, 20, 39]. The shifted separatrix mapping of the type (78) has been exploited to study magnetic field lines in tokamaks [12, 13, 40]. These studies also show that the separatrix map correctly reproduces the results of numerical integration of equations of motion.

9. Conclusion

The perturbation theory for Hamiltonian systems developed in this work gives a clear and rigorous way to construct Poincaré maps by means of symplectic mappings. It is actually a novel integration method for perturbed Hamiltonian equations. The method is based on a canonical coordinate transformation in the spirit of the Poincaré–von-Zeipel perturbation theory. However, unlike the latter classical perturbation theory based on the averaging principle and relying on the elimination of fast phases in the equations of motion, our approach uses a coordinate transformation which eliminates the perturbation in an entire period, while all perturbations act during one kick per period only. The dynamics of the transformed system during the entire period is determined by the unperturbed Hamiltonian. The relation between the solution before and after the kick is established by an inverse transformation to the old variables, thereby using their continuity. This procedure allows one to construct a Poincaré map for the original system by a symplectic map. It consists of three consecutive steps: (1) canonical transformation of variables to new variables; (2) evolution of new variables along unperturbed trajectories; (3) inverse canonical transformation to the old variables. Each of these steps is described by a symplectic mapping. We call this map *a symmetric symplectic map*.

It is clear that the symmetric map is written in terms of the original variables of the Hamiltonian system. This is the major advantage of the method as compared with the mapping method developed in [22, 23, 25]: this is because one does not need the symplectic correctors introduced in [26] in order to relate the mapping variables to the original ones. Moreover, unlike the latter method, our method does not encounter an integration across delta functions, which is not well-defined. On the other hand, in contrast to the classical perturbation methods, in our approach there is no problem with small denominators. Our map depends only on the natural parameters of the system and does not include any additional ones, such as an integration step etc.

The method allows us to study general Hamiltonian maps and their relation to continuous Hamiltonian systems. We have shown that the variables in many maps, studied in nonlinear

dynamics and chaos theory, e.g. the perturbed twist map, do not coincide with the variables of the corresponding continuous Hamiltonian systems. In particular, using the developed method we have studied the standard Hamiltonian (43), which has been a basic model for systems with a broad perturbation spectrum. It is widely accepted that to the system (43) there corresponds the standard map (44). It is shown that the variables in this map cannot be identified with the variables in the standard Hamiltonian, and we have derived a correct form of the map (called the symmetric standard map) in terms of the original variables.

In this paper we have presented only the basic elements of the new perturbation theory, and we have studied the foundation of the main Hamiltonian maps as they are widely used in nonlinear dynamics and chaos theory, like the perturbed twist mapping, the standard map and the separatrix map. We have also shown that the new method is in good agreement with the numerical integrations. Several problems concerning the stability of the new method, its accuracy, etc. were beyond the scope of the present paper, and require special investigation.

Acknowledgments

The author is grateful to Professor G Eilenberger for valuable comments and support. He also acknowledges stimulating discussions with Professor R Balescu, Professor D F Escande, Dr K H Finken, Dr W L Sadowski, Professor U Samm, Professor K H Spatschek and Professor G Wolf. He also wishes to thank Dr G Fuchs for careful reading of the manuscript and for correcting the English.

References

[1] Poincaré H 1992 New methods of celestial mechanics *History of Modern Physics and Astronomy* vol 13 (New York: AIP) ch 27, section 311
[2] Cuckenheimer J and Holmes P 1983 *Nonlinear Oscillations, Dynamical Systems, and Bifurcations of Vector Fields* (New York: Springer) p 22
[3] Lichtenberg A J and Lieberman M A 1983 *Regular and Stochastic Motion* (New York: Springer) ch 3
[4] Wiggins S 1990 Introduction to applied nonlinear dynamical systems and chaos *Texts in Applied Mathematics* (New York: Springer) section 1.2
[5] Arnold V I, Kozlov V V and Neishtadt A I 1988 Mathematical aspects of classical and celestial mechanics *Encyclopaedia of Mathematical Sciences. Dynamical Systems* vol 3 (Berlin: Springer) pp 138–82
[6] Meiss J D 1992 *Rev. Mod. Phys.* **64** 795–848
[7] Chirikov B V 1979 *Phys. Rep.* **52** 265
[8] MacKay R S and Meiss J D (ed) 1987 *Hamiltonian Dynamical Systems—A Reprint Selection* (Bristol: Hilger)
[9] Rechester A B and White R B 1980 *Phys. Rev. Lett.* **44** 1586–9
[10] Rechester A B, Rosenbluth M N and White R B 1981 *Phys. Rev.* A **23** 2664–72
[11] Greene J M 1984 Statistical physics and chaos in fusion plasmas *Non-Equilibrium Problems in the Physical Sciences and Biology* ed C W Norton Jr and L E Reichl (New York: Wiley) pp 3–20
[12] Abdullaev S S and Zaslavsky G M 1995 *Phys. Plasmas* **2** 4532–44
[13] Abdullaev S S and Zaslavsky G M 1996 *Phys. Plasmas* **3** 516–28
[14] Abdullaev S S, Finken K H, Kaleck A and Spatschek K H 1998 *Phys. Plasmas* **5** 196–210
[15] Balescu R, Vlad M and Spineanu F, 1998 *Phys. Rev.* E **58** 951–64
[16] Weiss J B and Knobloch E 1989 *Phys. Rev.* A **40** 2579–89
[17] Weiss J B 1991 *Phys. Fluids* A **3** 1379
[18] del-Castillo-Negrete D and Morrison P J 1993 *Phys. Fluids* A **5** 948–65
[19] Weiss J B 1994 *Physica* D **76** 230–8
[20] Ahn T and Kim S 1994 *Phys. Rev.* E **51** 2900–11
[21] Berg J S, Warnock R L, Ruth R D and Forest É 1994 *Phys. Rev.* E **49** 722–39
[22] Wisdom J 1982 *Astron. J.* **87** 577–93
[23] Wisdom J and Holman M 1991 *Astron. J.* **102** 1528–38
[24] Holman M and Wisdom J 1993 *Astron. J.* **105** 1987–99

[25] Touma J and Wisdom J 1994 *Astron. J.* **107** 1189–202
[26] Wisdom J, Holman M and Touma J 1996 Integration algorithms for classical mechanics *Fields Institute Communications* vol 10, ed J E Marsden, G W Patrick and W F Shadwick (Providence, RI: American Mathematical Society) pp 217–44
[27] Eberhard M 1998 Private communication
[28] Bogolyubov N N and Mitropol'skij Yu A 1958 *Asymptotic Methods in the Theory of Nonlinear Oscillations* 2nd edn (Moscow: Nauka) (Engl. Transl. 1961 New York: Gordon and Breach)
[29] Ali Nayfeh 1973 *Perturbation Methods* (New York: Wiley)
[30] Reichl L E 1992 *The Transition to Chaos in Conservative Classical Systems: Quantum Manifestations* Institute for Nonlinear Science (New York: Springer)
[31] Abdullaev S S, Finken K H and Spatschek K H 1999 *Phys. Plasmas* **6** 153–74
[32] Riedel K and Montvai A 1998 Private communication
[33] Filonenko N N and Zaslavsky G M 1968 *Sov. Phys.–JETP* **27** 851–7
[34] Escande D F 1988 Plasma theory and nonlinear and turbulent processes in physics *Proc. of the Int. Workshop (Kiev, 1987)* ed V G Bar'yakhtar *et al* (Singapore: World Scientific) pp 398–430
[35] Melnikov V K 1963 *Trans. Moscow Math. Soc.* **12** 1
[36] Abdullaev S S and Zaslavsky G M 1994 *Bull. Am. Phys. Soc.* **39** 1659
[37] Zaslavsky G M and Abdullaev S S 1995 *Phys. Rev.* E **51** 3901–10
[38] Abdullaev S S 1997 *Phys. Lett.* A **234** 281–90
[39] Lichtenberg A and Wood B 1989 *Phys. Rev.* A **39** 2153–9
[40] Abdullaev S S and Finken K H 1998 *Nucl. Fusion* **38** 531–44